

## Collapsing systems

A. Compagner, C. Bruin, and A. Roelse

*Laboratory of Applied Physics, Lorentzweg 1, 2628 CJ Delft, The Netherlands*

(Received 30 November 1988)

The stability problem posed in statistical mechanics by self-gravitating systems is discussed for the simpler case of systems with a purely attractive nonsingular pair potential of short range. Molecular-dynamics simulations of such systems are reported and are found to agree remarkably well with a modified version of the Hertel-Thirring cell model. A first-order phase transition is observed between a homogeneous phase at high energies and a collapsing phase with a single, very compact cluster in a diluted homogeneous background at low energies. The latter is not an extensive or thermodynamic phase. According to the cell model, really large systems are most likely to be found in a critical state hesitating between these two phases.

### I. INTRODUCTION

It is an ironic situation in statistical mechanics that the macroscopic properties of a system with a typical size of  $1 \text{ cm}^3$  usually are calculated by taking the limit in which the system becomes infinitely large, whereas in the case of extremely large systems, with sizes measured in light-years or parsecs, that limit cannot be employed at all. This is due to the stability condition which requires that the total potential energy  $\Phi$  of a system of  $N$  particles in a volume  $V$ , interacting through a pair potential  $\phi(r)$ , obeys

$$\Phi(\mathbf{r}_1, \dots, \mathbf{r}_N) = \frac{1}{2} \sum_{\substack{i,j \\ i \neq j}} \phi(|\mathbf{r}_i - \mathbf{r}_j|) \geq -N\epsilon, \quad (1)$$

for all possible positions  $\{\mathbf{r}_i\}$  of the particles, with  $\epsilon$  positive and independent of  $N$ . The statistical analogues of thermodynamic potentials like the entropy and the free energy then become extensive quantities in the thermodynamic limit, in which the volume  $V$  of the system increases with  $N$  to infinity, while the energy density or the temperature is kept constant. The role played by the thermodynamic limit in statistical mechanics has been discussed by many authors;<sup>1-4</sup> this limit is often equivalent to a properly defined continuum limit,<sup>5</sup> which fits better with the historical development of thermodynamics and in which the somewhat awkward notion of an infinitely large system is avoided.

For ordinary systems of particles, with a short-range pair potential that has a sufficiently hard core, the stability condition is satisfied. This is not so for a self-gravitating system of particles of mass  $m$ , with a pair potential

$$\phi(r) = -Gm^2/r, \quad (2)$$

$G$  being the universal gravitational constant. A statistical-mechanical description of such a system is therefore difficult, the more so because the long range of the gravitational potential and its singularity in the origin

are also a source of problems.

To describe gravothermal processes, astrophysicists and cosmologists have used a variety of techniques, ranging from phenomenological theories and numerical integrations of Fokker-Planck equations to Monte Carlo simulations and the numerical solution of Newtonian dynamics; see the reviews given by Spitzer<sup>6</sup> and Lynden-Bell.<sup>7</sup> The processes themselves vary from the birth of a planet or a star via the formation of globular star clusters or galaxies to the development of black holes or superclusters of galaxies. In general, a satisfactory description does not exist; it would often require elements from widely different branches of physics. In comparison with the resulting difficulties the invalidity of the stability condition for the gravitational potential is a minor problem.

To simplify even this problem, let us remove the singularity in the origin and the long range of the potential given in Eq. (2) by considering a hypothetical system with pair interaction

$$\phi(r) = -\epsilon \exp(-r^\delta/\sigma^\delta), \quad (3)$$

where  $\epsilon$  and  $\sigma$  are positive constants, while  $\delta$  is an even positive integer. This potential still violates the stability condition, and in the canonical ensemble a complete collapse of the system in the thermodynamic limit cannot be prevented: at constant temperature, all potential energy liberated when the particles coalesce into a single very dense cluster of size  $r \approx \sigma$  is irreversibly drained away by the heat bath. In the microcanonical ensemble, a complete collapse is opposed by an increasing amount of kinetic energy, so one is curious to see what happens.

In this paper the results of a molecular-dynamics study are presented for two-dimensional systems with  $\delta=4$  and 2, at various energies and densities. A new type of phase transition is observed, between a uniform phase with number density  $N/V$  at high energies and a collapsing phase with a single stable cluster of particles floating in a diluted homogeneous background at low energies. The latter phase, however, is not a thermodynamic phase in

the usual sense because it lacks the property of extensivity.

The occurrence of this phase transition does not depend on the dimensionality of the system. It may be noted that van Hove's theorem,<sup>8</sup> excluding the possibility of a phase transition for one-dimensional systems with short-range potentials, is not valid in the present case, due to the absence of a hard core in the pair potential. This could possibly be studied in detail for the particular case of a one-dimensional system with a purely attractive pair potential of rectangular shape, which may be exactly solvable. However, for systems of higher dimensionality exact solutions are impossible anyway.

To obtain some theoretical information for these cases, one of us (A.C.) studied some time ago a  $d$ -dimensional cell model in which the volume of the system is divided into a number of cells, each pair of particles within the same cell contributing a negative amount to the total potential energy. It turned out that the same model for  $d=3$  had been studied earlier by Hertel and Thirring.<sup>9</sup> Although the main results are similar, the differences in derivation, as well as interpretation and hence in some results, may justify that we include in this paper the  $d$ -dimensional version of the model, which is needed anyway for a comparison with the molecular-dynamics results.

$$Z(N, V, E) = \frac{1}{\hbar^{dN} N!} \int_V d\mathbf{r}_1 \cdots \int_V d\mathbf{r}_N \int_{-\infty}^{\infty} d\mathbf{p}_1 \cdots \int_{-\infty}^{\infty} d\mathbf{p}_N H(E - \Phi - K), \quad (5)$$

where  $\hbar$  is Dirac's constant,  $E$  the total energy of the system, and  $K = \sum_{i=1}^N p_i^2/2m$  the kinetic energy. The unit step function  $H(E - \Phi - K)$  restricts the integrations over the momenta to a  $dN$ -dimensional hypersphere with radius  $R = [2m(E - \Phi)]^{1/2}$ . The result of these integrations is just the volume  $(\pi^{1/2}R)^{dN}/\Gamma(\frac{1}{2}dN + 1)$  of this hypersphere. The integrations over the positions can be written as a sum over all possible distributions  $\{n_i\}$ , multiplied by a factor  $L^{dN}$ . One finds

$$Z(N, V, E) = \left[ \frac{2\pi m \epsilon L^2}{\hbar^2} \right]^{dN/2} \sum_{\{n_i\}}' \frac{\left[ \frac{E}{\epsilon} - \frac{1}{2}N + \frac{1}{2} \sum_{i=1}^M n_i^2 \right]^{dN/2}}{\Gamma(\frac{1}{2}dN + 1) \prod_{i=1}^M n_i!}, \quad (6)$$

where the factorial  $N!$  in the multinomial coefficients happened to cancel and where some factors were rearranged. The prime at the summation sign indicates that the restriction

$$\sum_{i=1}^M n_i = N \quad (7)$$

must be taken into account. The expression in parentheses containing  $E$  in Eq. (6) can never be negative; the smallest value that  $E$  can take is  $-\frac{1}{2}\epsilon N(N-1)$ , corresponding with  $N$  particles at rest in one cell.

## II. THE HERTEL-THIRRING MODEL REVISITED

Consider an isolated  $d$ -dimensional system of  $N$  particles with positions  $\mathbf{r}_i$  and momenta  $\mathbf{p}_i$  in a volume  $V$ , divided in  $M$  cells of size  $L^d$ , with  $V = ML^d$ . The number of particles in cell  $i$  is  $n_i$ . When two particles are in the same cell they contribute a negative amount  $-\epsilon$  to the potential energy, irrespective of their mutual distance in the cell. Particles in different cells do not interact.

The model is inspired by the treatment due to Ornstein and van Kampen<sup>10</sup> of the van der Waals gas, the difference being that the particles then are assumed to have a hard core, leading to the typical excluded-volume effect in the van der Waals equation of state. In the present case there is no repulsion between the particles whatsoever; all particles may reside in the same cell, this being opposed only by entropy.

For a given distribution  $\{n_i\}$  of the particles over the cells, the total potential energy is

$$\Phi(\{n_i\}) = -\frac{1}{2}\epsilon \sum_{i=1}^M n_i(n_i-1) = -\frac{1}{2}\epsilon \sum_{i=1}^M n_i^2 + \frac{1}{2}\epsilon N. \quad (4)$$

In the following it will be assumed that both  $N$  and  $n \equiv N/M$  are large, while  $M$  is not small.

The microcanonical partition function is

Abbreviating the prefactor in Eq. (6) as  $c^N$ , where  $c$  is a dimensionless constant, and the general term in the summation over  $\{n_i\}$  as  $\exp(N\psi)$ , we find a lower and an upper bound for the partition function

$$c^N \exp(N\psi_m) \leq Z \leq \mathcal{N} c^N \exp(N\psi), \quad (8)$$

where  $\psi_m$  is the maximum of  $\psi$  and where

$$\mathcal{N} = \binom{N+M}{M} \approx \left[ \frac{1}{n} (1+n)^{1+1/n} \right]^N \quad (9)$$

is the number of terms in the sum. The entropy  $S$ , per particle and divided by Boltzmann's constant  $k$ , can now also be sandwiched:

$$\ln c + \psi_m \leq \frac{S}{Nk} = \frac{\ln Z}{N} \leq \ln c + \psi + \frac{\ln \mathcal{N}}{N}. \quad (10)$$

The last term in the upper bound is negligible since  $n$  in Eq. (9) is assumed to be large. Hence the maximum term suffices.

Using Stirling's formula, omitting irrelevant contributions of order  $1/N$ , and redefining  $\psi$  by removing some terms together with  $\ln c$  to a new constant

$$\xi \equiv \frac{1}{2}d \ln \frac{2\pi m \epsilon L^2}{\hbar^2 d} + \frac{1}{2}d + 1 + (\frac{1}{2}d - 1) \ln N, \quad (11)$$

one finds

$$S/Nk = \xi + \psi_m, \quad (12)$$

where  $\psi_m$  is the maximum of

$$\psi \equiv \frac{1}{2}d \ln \left[ \eta + \sum_{i=1}^M v_i^2 \right] - \sum_{i=1}^M v_i \ln v_i \quad (13)$$

subject to the condition

$$\sum_{i=1}^M v_i = 1. \quad (14)$$

The relative occupation numbers  $v_i \equiv n_i/N$  were introduced, together with the quantity

$$\eta \equiv \frac{2E}{\epsilon N^2} - \frac{1}{N}, \quad (15)$$

where both terms are of the same order if  $E/\epsilon$  and  $N$  are so. The smallest value  $\eta = -1$  is reached when all particles are at rest in a single cell.

These expressions show that the thermodynamic limit, with  $N \rightarrow \infty$  at constant values of  $E/N$  and  $V/N$ , leads to difficulties. In the usual procedure the depth  $\epsilon$  and the range  $L$  of the pair potential are not changed in the limit, which implies that the number of cells  $M$  is proportional to  $N$ . The last term of  $\zeta$  can be added to  $\psi$ , giving

$$\psi' \equiv \frac{1}{2}d \ln \left[ N\eta + N \sum_{i=1}^M v_i^2 \right] - \sum_{i=1}^M v_i \ln(Nv_i). \quad (16)$$

If the maximum  $\psi'_m$  of this quantity occurs at the uniform distribution  $v_i = 1/M$  there is no problem:  $\psi'_m$  is constant in the limit, because  $N\eta$  and  $N/M$  are so. The entropy then is an extensive quantity. When, however, the maximum would correspond with a nonuniform distribution, this is no more true.

While restricting their attention to the case  $d = 3$ , Hertel and Thirring<sup>9</sup> avoid this problem by assuming that  $M = V/L^d$  is constant for  $N \rightarrow \infty$  at constant values of  $E/N$  and  $V/N$ , whereas  $\epsilon$  is taken to be proportional to  $1/N$ . This "scaling procedure," as it will be called here, is similar to the limit of an infinitely weak interaction of infinitely long range used in the Kac-Uhlenbeck-Hemmer study<sup>11</sup> of a one-dimensional van der Waals fluid. Since  $\eta$  and  $M$  now are constant, the maximalization of  $\psi$  is independent of  $N$ . The stability condition is restored by this procedure, and the entropy is an extensive quantity under all circumstances. This holds for any value of  $d$ . It may be verified that in Eq. (11) the troublesome last term of  $\zeta$  now can be combined with the first term into a quantity which is constant in the limit.

In the Kac-Uhlenbeck-Hemmer study the scaling procedure is necessary to obtain a phase transition in the one-dimensional van der Waals system. In the present case a phase transition always occurs (irrespective of the dimensionality of the system) due to the purely attractive pair potential; the scaling procedure is only needed to maintain extensivity. From a physical point of view the scaling procedure is unwanted, because it removes the cosmological implications from the model, or simply because it is undesirable to manipulate the pair potential for calculational purposes only. It will not be used here; it is sufficient to assume that  $N$  is large but finite.

### III. FINDING THE MAXIMUM

In  $M$ -dimensional  $\{v_i\}$  space Eq. (14), together with  $0 \leq v_i \leq 1$ , defines an  $(M-1)$ -dimensional simplex. The maximum of  $\psi$  cannot occur along the boundaries of this simplex, where at least one particular  $v_i$  vanishes: due to the second term in Eq. (13), at least one derivative  $\partial\psi/\partial v_i$  is then infinite. When  $\eta$  is negative, another restriction follows from

$$\eta + \sum_{i=1}^M v_i^2 \geq 0, \quad (17)$$

where  $\eta \geq -1$  holds. The value  $\eta = -1$  corresponds with a complete collapse at zero temperature, with  $v_i = 1$  for one of the cells. At the boundaries due to Eq. (17), the first term in Eq. (13) gives  $\psi = -\infty$ .

The maximum of  $\psi$  can thus be found by differentiation. Equation (14) is incorporated by eliminating  $v_M$ ,

$$\psi = \frac{1}{2}d \ln \left[ \eta + \sum' v_i^2 + \left[ 1 - \sum' v_i \right]^2 \right] - \sum' v_i \ln v_i - \left[ 1 - \sum' v_i \right] \ln \left[ 1 - \sum' v_i \right], \quad (18)$$

where the prime means summation from  $i=1$  to  $i=M-1$ ; when the prime is omitted the term  $i=M$  will be included. The stationary points obey

$$\frac{\partial\psi}{\partial v_i} = \frac{d(v_i - v_M)}{\eta + \sum v_i^2} - \ln \frac{v_i}{v_M} = 0 \quad (19)$$

for  $i=1, \dots, M-1$ , where  $v_M$  was reintroduced for short. The homogeneous case  $v_i = v_M = 1/M$  for all  $i$  is always a solution, unless it violates Eq. (17). Other stationary points are found by rewriting Eq. (19) for all values of  $i$  for which  $v_i \neq v_M$  holds:

$$\frac{d v_M}{\eta + \sum v_i^2} = \frac{1}{v_i/v_M - 1} \ln \frac{v_i}{v_M}. \quad (20)$$

When  $\{v_i\}$  is a solution, the left-hand side has a fixed value, and since the right-hand side is monotonous, only one value for  $v_i/v_M \neq 1$  can occur. There is no loss of generality when we assume that the additional stationary points obey, possibly after renumbering,

$$0 < v_1 = v_2 = \dots = v_q < v_{q+1} = v_{q+1} = \dots = v_M < 1, \quad (21)$$

with  $0 \leq q \leq M-1$ .

Replacing  $v_M$  in Eq. (19) again by  $\sum'(1-v_i)$ , one finds for the elements of the  $(M-1) \times (M-1)$  matrix  $\Psi$  of second derivatives:

$$\Psi_{jk} \equiv \frac{\partial^2\psi}{\partial v_j \partial v_k} = \frac{d}{\eta + \sum v_i^2} (1 + \delta_{jk}) - \frac{2d(v_j - v_M)(v_k - v_M)}{(\eta + \sum v_i^2)^2} - \frac{1}{v_j} \delta_{jk} - \frac{1}{v_M}, \quad (22)$$

where Kronecker's  $\delta$  symbol was used. For short, the quantities

$$\begin{aligned} r &\equiv \frac{d}{\eta + \sum v_i^2} - \frac{1}{v_1}, \\ s &\equiv \frac{d}{\eta + \sum v_i^2} - \frac{1}{v_M}, \\ t &\equiv \frac{-2d(v_1 - v_M)^2}{(\eta + \sum v_i^2)^2}, \end{aligned} \tag{23}$$

$$a \equiv r + s + t - \lambda, \quad b \equiv s + t, \quad c \equiv 2s - \lambda \tag{24}$$

are introduced,  $\lambda$  being an eigenvalue. The characteristic equation is

$$D(q; q') \equiv |\Psi - \lambda I| = 0, \tag{25}$$

with  $q' = M - 1 - q$ , while  $I$  is the unit matrix. The determinant has the following symmetric form, in which the first  $q$  rows and columns are slightly separated from the remaining ones:

$$D(q; q') = \begin{vmatrix} a & b & \cdot & \cdot & b & s & \cdot & \cdot & \cdot & s \\ b & & & & \cdot & \cdot & & & & \cdot \\ \cdot & & & & \cdot & \cdot & & & & \cdot \\ \cdot & & & & b & \cdot & & & & \cdot \\ b & \cdot & \cdot & \cdot & b & a & s & \cdot & \cdot & s \\ s & \cdot & \cdot & \cdot & \cdot & s & c & s & \cdot & s \\ \cdot & & & & \cdot & \cdot & s & \cdot & & \cdot \\ \cdot & & & & \cdot & \cdot & \cdot & \cdot & & \cdot \\ \cdot & & & & \cdot & \cdot & \cdot & \cdot & & s \\ s & \cdot & \cdot & \cdot & \cdot & s & s & \cdot & \cdot & s & c \end{vmatrix}. \tag{26}$$

Subtracting the second column and row from the first ones, and repeating this process  $q - 1$  times, we find

$$D(q; q') = q(a - b)^{q-1} D(1; q') - (q - 1)(a - b)^q D(0; q'). \tag{27}$$

With  $D(0; 1) = c$  and  $D(0; 0) = 1$  we get

$$D(1; q') = (a + c - 2s) D(0; q') - (s - c)^2 D(0; q' - 1), \tag{28}$$

$$D(0; q') = (c - s)^{q'-1} [(q' - 1)s + c]. \tag{29}$$

Insertion into Eq. (27) and use of Eqs. (24) leads to

$$\begin{aligned} D(q; M - q - 1) &= (r - \lambda)^{q-1} (s - \lambda)^{M - q - 2} \\ &\times [\lambda^2 - \lambda(Ms + qt + r) \\ &+ (M - q)(qt + r)s + qs^2]. \end{aligned} \tag{30}$$

To correspond with a maximum all  $M - 1$  eigenvalues must be negative in the stationary point. Consider the eigenvalue  $\lambda = s$ . Using Eqs. (20) and (23) one finds

$$\lambda v_M = s v_M = \frac{d v_M}{\eta + \sum v_i^2} - 1 = \frac{1}{v_1/v_M - 1} \ln \frac{v_1}{v_M} - 1, \tag{31}$$

where  $v_1 < v_M$  holds. The function  $\ln y / (y - 1)$  is, however, always larger than 1 for  $y < 1$ . Hence the eigenvalue  $\lambda = s$  is always positive in the stationary point. Similarly,  $\lambda = r$  is found to be always negative. It follows that all factors  $s - \lambda$  in Eq. (30) must disappear; this happens for  $q = M - 2$  and  $q = M - 1$ :

$$\begin{aligned} D(M - 2; 1) &= (r - \lambda)^{M-3} \\ &\times [\lambda^2 - \lambda(Ms + Mt - 2t + r) \\ &+ 2(Mt - 2t + r)s + (M - 2)s^2], \end{aligned} \tag{32}$$

$$D(M - 1; 0) = (r - \lambda)^{M-2} [(M - 1)s + (M - 1)t + r - \lambda]. \tag{33}$$

Writing the quadratic form in Eq. (32) as  $\lambda^2 - A\lambda + B$  one finds that  $B/s = 2A - (M + 2)s$  holds. This means that  $A < 0$  and  $B > 0$  cannot be true simultaneously,  $s$  still being positive. The two solutions  $\lambda_{\pm}$  of  $\lambda^2 - A\lambda + B = 0$  then cannot both be negative: Eq. (32) can never correspond to a maximum. It should be noted, however, that the existence of positive eigenvalues close to zero cannot be excluded, indicating long relaxation times in the dynamics of the model; this may also happen for smaller values of  $q$ .

The only remaining possibility is Eq. (33), which corresponds with a maximum when

$$\lambda = (M - 1)s + (M - 1)t + r < 0 \tag{34}$$

holds. This leads to the inhomogeneous solution, with  $v_i = v_1 < v_M$  for  $i = 1, \dots, M - 1$ . In equilibrium, any inhomogeneity that may occur is restricted to a single cell with an increased occupation number to which all other cells contribute in equal amounts.

#### IV. THE HOMOGENEOUS PHASE

The homogeneous solution  $v_i = v_M$  for all  $i$  is in fact still contained in Eq. (34): put  $s = r$  and  $t = 0$ , and note that Eqs. (20) and (31) are invalid in this case. The resulting characteristic equation,  $(r - \lambda)^{M-2}(Mr - \lambda) = 0$ , also follows from Eq. (30) by putting  $q = 0$  and  $s = r$ . The requirement  $s = r < 0$  for  $v_i = 1/M$  gives rise to the energy condition

$$\eta > \eta_h \equiv (d - 1)/M, \tag{35}$$

which is stronger than Eq. (17). When Eq. (35) holds, the homogeneous solution corresponds to at least a local maximum,

$$\psi_m = \frac{1}{2}d \ln \left[ \eta + \frac{1}{M} \right] + \ln M . \quad (36)$$

All properties of the homogeneous phase follow from

$$\begin{aligned} \frac{S}{Nk} &= \frac{1}{2}d \ln \frac{2\pi m \epsilon L^2}{\hbar^2 d} + \frac{1}{2}d + 1 + (\frac{1}{2}d - 1) \ln N \\ &+ \frac{1}{2}d \ln \left[ \eta + \frac{1}{M} \right] + \ln M . \end{aligned} \quad (37)$$

The temperature and the specific heat are

$$T \equiv \frac{1}{\partial S / \partial E} = \frac{\epsilon N}{kd} \left[ \eta + \frac{1}{M} \right] , \quad (38)$$

$$C_V \equiv \frac{1}{\partial T / \partial E} = \frac{1}{2}d N k . \quad (39)$$

Using Eq. (15) one finds that Eq. (38) is equivalent with  $E = K + \Phi$ , where  $K = \frac{1}{2}d N k T$  is the kinetic energy of the system and  $\Phi = -(\epsilon N^2 / 2M) + \frac{1}{2}\epsilon N$  the potential energy. In the homogeneous phase the specific heat at constant volume is that of an ideal gas, as could be expected. The above results agree with those obtained by Hertel and Thirring<sup>9</sup> for the case  $d=3$ , although the derivations differ.

At constant linear cell size  $L$ , which is a measure for the range of an effective pair potential between the particles, the pressure is

$$p_L \equiv T \frac{\partial S}{\partial V} \Big|_L = \frac{\epsilon N^2}{ML^d d} \left[ \eta - \frac{d-2}{2M} \right] . \quad (40)$$

Hertel and Thirring<sup>9</sup> do not calculate the pressure explicitly, but note that it is always equal to the ideal-gas pressure  $NkT/V$ . Apparently, they differentiated with respect to  $V = ML^d$  by varying  $L$  at constant  $M$ . For general  $d$  their results would be

$$p_M \equiv T \frac{\partial S}{\partial V} \Big|_M = \frac{\epsilon N^2}{ML^d d} \left[ \eta + \frac{1}{M} \right] , \quad (41)$$

which in view of Eq. (38) is indeed identical to  $p_M = NkT/V$ . In this interpretation, in which the cell volume varies with  $V$ , the potential energy cannot contribute to the work done on the system.

Using the equations in this section it is easy to show that the homogeneous phase has the property of extensivity, irrespective of whether in the thermodynamic limit the usual procedure is followed or the scaling procedure. From a physical point of view, homogeneity is indeed a sufficient prerequisite of extensivity.

## V. THE COLLAPSING PHASE

The only other possibility for a (local) maximum  $\psi_m$  of the entropy function  $\psi$  occurs when Eq. (34) holds in combination with an  $(M-2)$ -fold degenerate eigenvalue  $\lambda = r < 0$ . In this case,  $v_i = v_1 < M^{-1} < v_M$  must hold for  $i = 1, \dots, M-1$ . Incorporating this condition into  $\psi$  one finds

$$\begin{aligned} \psi &= \frac{1}{2}d \ln [ \eta + (M-1)v_1^2 + v_M^2 ] \\ &- (M-1)v_1 \ln v_1 - v_M \ln v_M . \end{aligned} \quad (42)$$

The stationarity condition now reads

$$\frac{d(v_M - v_1)}{\eta + (M-1)v_1^2 + v_M^2} = \ln \frac{v_M}{v_1} , \quad (43)$$

where  $(M-1)v_1 + v_M = 1$  is understood. Substitution of  $x = v_M/v_1$  and elimination of  $v_1$  leads to

$$\eta = \frac{d(x-1)}{(M-1+x) \ln x} - \frac{M-1+x^2}{(M-1+x)^2} , \quad (44)$$

with

$$x = (M-1)v_M / (1-v_M) . \quad (45)$$

These equations determine  $\eta$  as a function of  $v_M$ . The inverse function gives for each  $\eta$  the value or values of  $v_M$  for which  $\psi$  is stationary. Upon insertion into Eq. (42) the values that maximize  $\psi$  are found; they are denoted by  $v_M^0(\eta)$ .

This solution turns out to have two branches; one for  $\eta > \eta_h$  with  $v_M^0 = 1/M$ , corresponding to the homogeneous phase; and one for  $\eta$  below a critical value  $\eta_c$  (larger than  $\eta_h$ ) with  $v_M^0 > 1/M$ , corresponding to the collapsing phase. Between  $\eta_h$  and  $\eta_c$  the two maxima coexist; they are equally large for  $\eta = \eta_t$ , which is taken as the location of the true phase transition. Below  $\eta_t$  the homogeneous phase is metastable (its maximum being the smaller of the two), and above  $\eta_t$  the collapsing phase is so. The relation  $0 \leq \eta_h < \eta_t < \eta_c$  holds for all finite values of  $M$ , the equal sign referring exclusively to the case  $d=1$ . In the limit  $M \rightarrow \infty$  not only  $\eta_h$  vanishes, as it should according to Eq. (35), but also  $\eta_t$  and  $\eta_c$  vanish. The behavior of these quantities is sketched in Fig. 1 for the case  $d=2$ .

The dependence of the function  $v_M^0(\eta)$  on  $E$  and  $N$  is completely contained in  $\eta$ , apart from  $N \gg M$ , which is always understood. It is shown in Fig. 2 for three widely different values of  $M$ , again for  $d=2$ . The dependence on  $M$  of this function is seen to be rather weak. For  $M=20$  (too small a value for the maximum-term method to be reliable) the homogeneous branch is included, together with the tie lines at  $\eta_h$ ,  $\eta_t$ , and  $\eta_c$ ; the occurrence of these tie lines for finite systems is of course due to the maximum-term method. For  $M=10^4$  only the branch of the collapsing phase is shown, ending at  $\eta = \eta_c$  with a vertical slope. The third curve in the figure, restricted to the domain  $-1 \leq \eta \leq 0$ , is the asymptote

$$\lim_{M \rightarrow \infty} v_M^0(\eta) = (-\eta)^{1/2} , \quad (46)$$

which does not depend on  $d$ . This asymptote follows

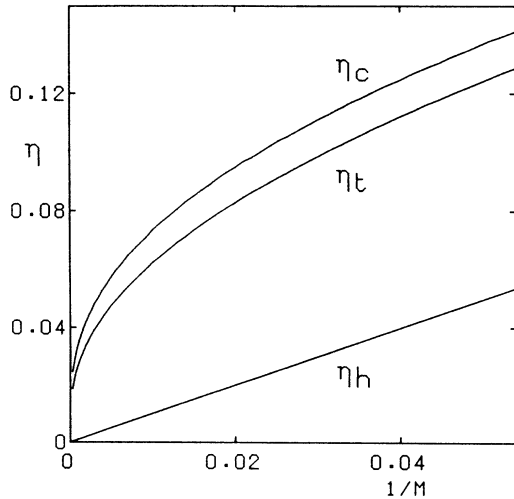


FIG. 1. The end points  $\eta_h$  and  $\eta_c$  of the metastable branches and the transition point  $\eta_t$  are shown as functions of the inverse number of cells, for the two-dimensional cell model. The straight line for  $\eta_h$  obeys Eq. (35).

directly from Eq. (43), as shown in Sec. VIII as part of a general discussion of the limit  $M \rightarrow \infty$  (at a constant value of  $N/M$ ). In the meantime, the system is still taken to be large but finite.

Once  $v_M^0(\eta)$  is known for the collapsing phase, the entropy of that phase is known, and the temperature and pressure are found by differentiations with respect to  $\eta$  and  $M$ . Because of stationarity the derivatives of  $v_M^0(\eta)$

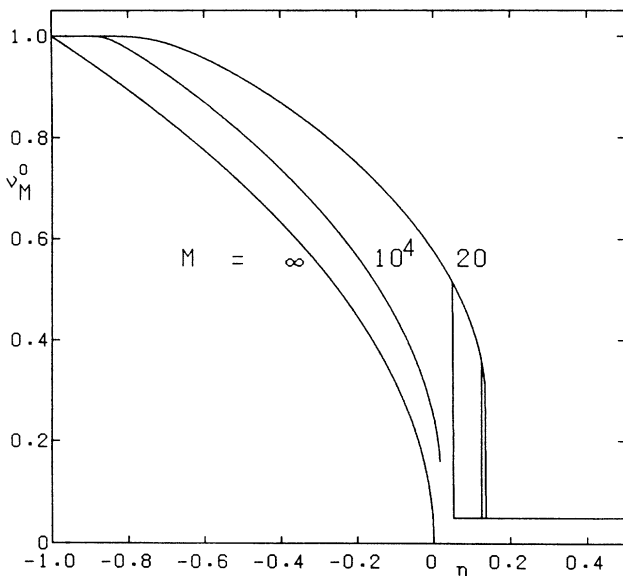


FIG. 2. The degree of occupation  $v_M^0(\eta)$  which maximizes the entropy of the two-dimensional cell model for a few values of  $M$ . For  $M=20$  the homogeneous solution  $v_M^0=1/M$  is included and the tie lines at  $\eta_h$ ,  $\eta_t$ , and  $\eta_c$  are shown. The curve for  $M=\infty$  is the asymptote given by Eq. (46).

do not appear. The results are

$$\begin{aligned} \frac{S}{Nk} = & \frac{1}{2}d \ln \frac{2\pi m \epsilon L^2}{\hbar^2 d} + \frac{1}{2}d + 1 + (\frac{1}{2}d - 1) \ln N \\ & + \frac{1}{2}d \ln \left[ \eta + \frac{1-2\nu + M\nu^2}{M-1} \right] \\ & - (1-\nu) \ln \frac{1-\nu}{M-1} - \nu \ln \nu, \end{aligned} \quad (47)$$

$$T = \frac{\epsilon N}{kd} \left[ \eta + \frac{1-2\nu + M\nu^2}{M-1} \right], \quad (48)$$

$$p_L = \frac{\epsilon N^2(1-\nu)}{dL^d(M-1)} \left[ \eta + \frac{1-2\nu + M\nu^2}{M-1} - \frac{d(1-\nu)}{2(M-1)} \right]. \quad (49)$$

In these equations  $\nu$  is short for  $v_M^0(\eta)$ . For  $d=3$ , they are identical to the results of Hertel and Thirring<sup>9</sup> for the collapsing phase, except for the pressure; their interpretation would not lead to  $p_L$  but to

$$p_M = \frac{\epsilon N^2}{dL^d M} \left[ \eta + \frac{1-2\nu + M\nu^2}{M-1} \right], \quad (50)$$

which in view of Eq. (48) is still equal to the ideal-gas pressure. Since  $M$  is always assumed to be large, the main difference between  $p_L$  and  $p_M$  is the factor  $1-\nu$  in Eq. (49). Varying  $L$  at stationarity leaves the distribution over the cells intact, which indeed implies that only the kinetic degrees of freedom contribute to the pressure; their influence is contained in the first terms of Eqs. (37) and (47), the only terms where  $L$  appears.

Strictly speaking, by renumbering the cells we introduced an  $M$ -fold degeneracy for the maximum, corresponding to the collapsed phase. The lower bound on  $Z$  in Eq. (8) should therefore be multiplied by a factor  $M$ . The extra term  $\ln M/N$  that would have to be added to Eq. (47) is usually negligible. Another remark concerns the appearance of the factors  $N$  and  $N^2$  in Eqs. (48)–(50): they should be seen in relation to the  $N$  dependence of  $\eta$ . However, the collapsing phase is not extensive; see Sec. VIII, where the asymptotic properties of the cell model are discussed.

The inverse of the specific heat is the derivative of  $T$  with respect to  $E$ , that is, with respect to  $\frac{1}{2}\epsilon N^2 \eta$ , but now the derivative of  $v_M^0$  with respect to  $\eta$  enters:

$$\frac{1}{C_V} = \frac{2}{Nkd} \left[ 1 + \frac{2(M\nu-1)}{M-1} \frac{\partial \nu}{\partial \eta} \right]. \quad (51)$$

It is easily verified that Eqs. (37)–(41) are retrieved by putting  $\nu=1/M$  in the above equations.

Curves showing the behavior of these quantities for the typical case  $d=2$  will be given in Sec. VII as part of the comparison with the molecular-dynamics results for a system with a true pair potential. In anticipation, a rather unusual feature of the collapsing phase is discussed here. Referring to Eqs. (38) and (48), we note that  $T$  is small in two cases: in the homogeneous phase for  $\eta$  positive but small, and in the collapsing phase for  $\eta \approx -1$ ,

when the collapse is almost complete. The slope of  $T(\eta)$  corresponds with that for an ideal gas in both cases; indeed, in both cases the potential energy is constant. In between,  $T$  shows a maximum, corresponding to an infinite specific heat, at a value of  $\eta$  well inside the collapsing phase. When  $\eta$  approaches this value from above the specific heat is negative: more particles fall into the collapsing cluster and the mean kinetic energy increases.

A negative specific heat is a common phenomenon in astrophysics (see the discussion by Lynden-Bell<sup>7</sup>), but in statistical mechanics it is almost anathema because the equivalence of the microcanonical and the canonical ensemble in the thermodynamic limit holds only for states with a positive specific heat, just as the equivalence in the limit of the canonical and the grand ensemble is only true for states with a positive isothermal compressibility. Indeed, in the canonical ensemble the specific heat is essentially equal to the variance of the total energy, which is positive by definition. For finite systems the microcanonical and the canonical ensemble lead to different thermodynamic quantities, although the canonical partition function by being the Laplace transform of the microcanonical partition function contains the same mathematical information as the latter as long as all terms of  $Z(N, V, E)$  are taken into account. It is especially the information pertaining to states with negative specific heat which in the thermodynamic limit (taken in the usual manner or according to the scaling procedure) cannot be carried over to the canonical ensemble; this is also true when instead of the limit the maximum-term method is used, which does not require that the system be strictly infinite. For the present system the use of the canonical ensemble would exclude the most interesting states and must be sacrificed, which is only fitting for a model with cosmological pretensions: one cannot put the universe into a heat bath.

## VI. THE SIMULATED SYSTEM

Does the cell model describe the properties of a hypothetical system of purely attractive particles, with a true pair potential like that of Eq. (3)? Since the particles are imaginary, only computer experiments can tell. Using the molecular-dynamics method we studied a two-dimensional system of  $N$  particles in a periodic box of volume  $V$ , for two different system sizes ( $N = 132, 600$ ) at four different densities ( $\rho^* = 0.64, 0.29, 0.13, \text{ and } 0.03$ ). The potential of Eq. (3) was used with  $\delta = 2$  or  $\delta = 4$ . This potential was cut off at the distance  $R = 3\sigma$ . As a function of the total energy we determined the temperature, the pressure, and the specific heat by averaging the appropriate expressions over the trajectory in phase space generated during a measuring run.

For completeness, these expressions are given explicitly in terms of the velocities  $v_i$  and positions  $r_i$  of the particles:

$$K = \frac{1}{2}m \sum_{i=1}^N v_i^2, \quad (52)$$

$$P = \frac{2K}{dV} - \frac{1}{dV} \sum_{\substack{i,j \\ i < j}}^N \mathbf{r}_{ij} \cdot \frac{\partial \Phi}{\partial \mathbf{r}_{ij}}, \quad (53)$$

where  $\mathbf{r}_{ij}$  is short for  $\mathbf{r}_i - \mathbf{r}_j$  and where  $K$ ,  $P$ , and  $\Phi$  are, respectively, the kinetic energy, the mechanical pressure, and the potential energy. The temperature and the thermodynamical pressure follow directly from  $T = \langle K \rangle / \frac{1}{2}dNk$  and  $p = \langle P \rangle$ , the brackets indicating time averages over the trajectory generated in a run. In molecular-dynamics experiments, at constant value of the total energy  $E = \langle K \rangle + \langle \Phi \rangle$ , the specific heat follows from

$$\frac{Nk}{C_V} = \frac{2}{d} - \frac{4}{d^2 N k^2 T^2} (\langle K^2 \rangle - \langle K \rangle^2), \quad (54)$$

as was first shown by Lebowitz, Percus, and Verlet.<sup>12</sup> There is no *a priori* reason why this quantity should be positive. In the equation,  $K$  could be replaced by  $\Phi$ , their variances being equal in the microcanonical ensemble. As mentioned, we adopted  $d = 2$  in the simulations.

The calculations were performed on the Delft molecular-dynamics processor (DMDP) built by Bakker,<sup>13</sup> a special-purpose machine which because of its speed and continuous availability is very suitable for this problem in view of the relatively long relaxation times that were encountered. Each measuring run consisted of  $\approx 10^5$  sufficiently small time steps for the numerical integration of Newton's equations and took 2 to 3 h on the DMDP. The initial conditions for a measuring run were obtained in a relaxation run of  $\approx 10^6$  time steps, taking about the same amount of real time as a measuring run because less interaction with the host computer was required. For the initial conditions of a relaxation run the final conditions of the previous measuring run were used, after energy adjustment by scaling the particle velocities. Both "heating" and "cooling" sequences of measuring runs were carried out.

The use of the DMDP also implied a restriction: in this machine the usual linked-list method of molecular dynamics is employed, but the linked lists can contain at most 256 particles. This length is sufficient for Lennard-Jones systems or other systems involving a hard core in the pair potential, but when the largest system studied here, with  $N = 600$ , enters the collapsing phase the list soon overflows, making a correct simulation impossible. This problem could be circumvented by using a general-purpose computer, but for  $N \gtrsim 1000$  the relaxation times would probably become too long anyway, in particular at low densities.

For a quantitative comparison of the cell model with the simulated system the parameters must be identified. For the depth of the potential well we adopted already  $-\epsilon$  in both cases. The spatial scales can be fixed by identifying the location of the inflection point of  $\phi(r)$  as given by Eq. (3) with the position of the cell boundary of the cell model  $r = 0$  referring to the middle of the cell. The inflection point occurs at

$$(r/\sigma)^\delta = \frac{\delta - 1}{\delta}, \quad (55)$$

that is, at  $r/\sigma \approx 0.71$  for  $\delta = 2$  and at  $r/\sigma \approx 0.93$  for  $\delta = 4$ . The ratio  $L/\sigma$ , where  $L$  is the linear cell size, should be twice these values; we adopted  $L/\sigma = 1.42$  for  $\delta = 2$  and  $L/\sigma = 1.86$  for  $\delta = 4$ , with more than sufficient accuracy, given the weak dependence on  $M$  of the cell

model. It may be noted also that a central potential does not fit into a square box without ambiguity.

There are no other parameters that can be adjusted. In the comparison reduced quantities are employed, defined by

$$T^* = \frac{kT}{\epsilon}, \quad \rho^* = \frac{N\sigma^2}{V}, \quad p^* = \frac{pV}{\epsilon N}, \quad C_V^* = \frac{C_V}{Nk}, \quad (56)$$

where  $\rho^*$  is the reduced density. Notice that the number of cells  $M = V/L^2$  of the cell model follows from the reduced density by means of

$$M = \frac{N\sigma^2}{\rho^* L^2} = \begin{cases} 0.50N/\rho^* & \text{for } \delta=2, \\ 0.29N/\rho^* & \text{for } \delta=4. \end{cases} \quad (57)$$

For the energy, the parameter  $\eta$  defined in Eq. (15) will be used. The inclusion of the term  $-1/N$  guarantees that both for the cell model and for the simulated system the completely collapsed state always occurs at  $\eta = -1$  with  $T^* = 0$ , irrespective of  $N$ . The ground state of the system, in which all particles are almost at rest at the bottom of their collective well, can be interpreted as that of a system of independent particles moving in a collective quasiexternal field. In the Appendix it is shown that  $T^*$  increases linearly for an initial increase of  $\eta$  beyond its absolute minimum; in particular, for  $d=2$  the following relations, valid for  $\eta \searrow -1$ , are found immediately from Eq. (A5):

$$T^* = \frac{1}{2}N \frac{\delta}{\delta+2} (\eta+1), \quad (58)$$

$$C_V^* = 1 + \frac{2}{\delta}. \quad (59)$$

For  $\delta = \infty$  the pair potential of Eq. (3) is a rectangular well. Then, the collective field in the ground state is also a rectangular well, and the system behaves as an ideal gas. The same ground state occurs in the cell model; the last two equations, with  $\delta = \infty$ , must hold also in that case.

To see how the general properties of systems of purely attractive particles depend on the shape of the pair potential it may be interesting to do simulations with larger (even) values of  $\delta$  than employed here. One could also experiment with altogether different shapes of the attractive pair potential, although for practical reasons they should remain to be nonsingular and of short range.

## VII. SIMULATION RESULTS

During a simulation run at a particular value of  $\eta$ , a small number of momentary configurations obtained in the DMDP were transferred to the host computer for display or for further analysis. One of these configurations, at  $\eta = 0.035$ , is shown in Fig. 3. The size of the circles representing the particles is such that the centers of two circles just in contact are a distance  $r = 0.93\sigma$  (for  $\delta = 4$ ) apart, corresponding with the inflection point of the pair potential given by Eq. (55). The particle diameter thus is equal to  $\frac{1}{2}L$ , half the cell size of the cell model with which the system will be compared.

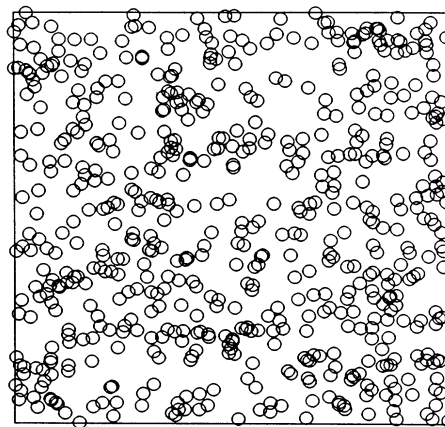


FIG. 3. A typical configuration in the homogeneous phase during a simulation at  $\eta = 0.035$  of a system of  $N = 600$  particles with the pair potential of Eq. (3) for  $\delta = 4$ . The reduced density is  $\rho^* = 0.64$ . The diameter of the particles is given by Eq. (55). The chainlike structures are not completely random, but also very unstable.

The chainlike structures apparent in Fig. 3 turn out to have a very transient nature and do not indicate the presence of bound states: the system is in the homogeneous phase. These structures are largely accidental (the eye discovers similar structures in completely random configurations), but a detailed cluster analysis reveals the presence of small correlations, in particular upon approaching the collapsing phase. This premonitory phenomenon turns up also in the temperature (see below).

When the energy is decreased sufficiently, a sudden transition is observed in which the system, passing sometimes through a transient state with two or more clusters, ends up in a state with a single compact cluster floating slowly around in a diluted homogeneous background: the collapsing phase is entered. A typical configuration is shown in Fig. 4. The collapsing cluster is very stable, al-

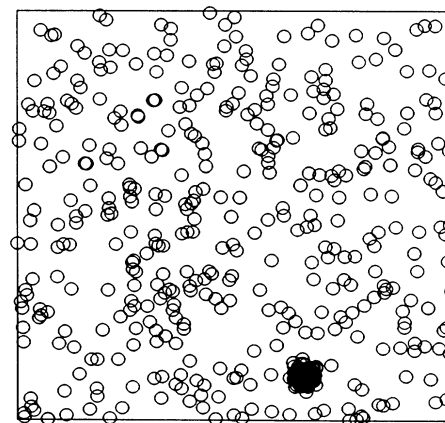


FIG. 4. A typical configuration of the same system as in Fig. 3, but now at  $\eta = 0.015$ , in the collapsing phase. The cluster contains 192 particles and is stable, apart from minor fluctuations.



though a steady exchange of individual particles with the background takes place. Upon formation it immediately contains a sizable fraction of all particles, indicating that the phase transition is of first order, resembling condensation. The new phase is not a bulk phase, however, the size of the collapsing cluster being of the same order as the size of the particles. Due to the absence of a hard core the collective potential inside a cluster cannot be saturated, and this is why the collapsing phase cannot be extensive.

The first-order character of the transition is confirmed by the behavior of the thermodynamic quantities and by the appearance of metastable states: in series of runs with decreasing or increasing  $\eta$  (indicated with “cooling” or “heating” in some of the figures below) a rather narrow region just above  $\eta=0$  was encountered where the two phases overlap. A precise determination of the end-points of the metastable branches was difficult because of the long lifetimes involved.

The configurations were analyzed numerically by adapting a method due to Stoddard<sup>14</sup> to our purposes, which lead to the number of particles  $N_c$  in the largest “connected” cluster for each configuration. In the homogeneous phase this number was always small, though somewhat arbitrary (depending on a “connectivity distance”). In the collapsing phase,  $N_c$  as determined by the method has a precise meaning and, upon inspection, was found to agree with the number of particles in the collapsing cluster. The data points in Fig. 5 give the quantity  $v=N_c/N$ , averaged over 11 different configurations for each value of  $\eta$ , for the same system of 600 particles as in

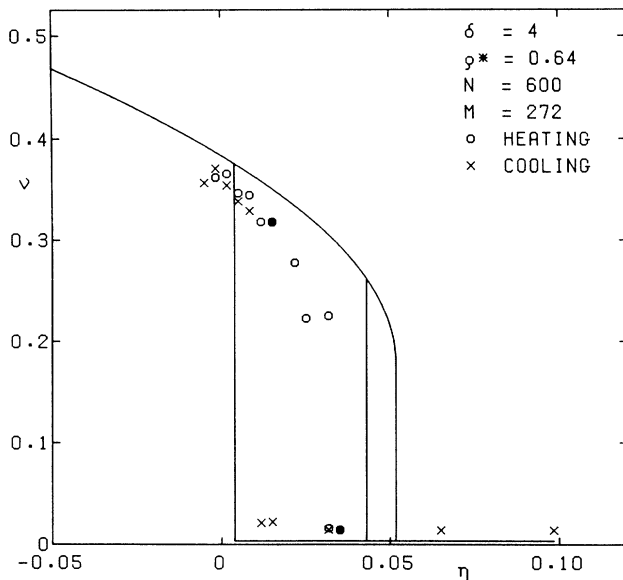


FIG. 5. The data points show  $v=N_c/N$ , the relative number of particles in the largest cluster averaged over 11 different configurations at each  $\eta$ , for the system as indicated. The solid line is  $v_M^0(\eta)$  of the corresponding cell model, including the tie lines. The black dots indicate the runs of the “heating” sequence during which the configurations of Figs. 3 and 4 occurred.

the preceding two figures; because of the linked-list overflow no data were obtained for  $\eta < -0.01$ . The solid line shows  $v_M^0$  of the corresponding cell model, with  $M$  given by Eq. (57), including the tie lines at  $\eta_h$ ,  $\eta_t$ , and  $\eta_c$  (in general, the region of metastabilities seems to be somewhat larger for the cell model than for the simulated systems). The same quantities are compared in Fig. 6 for a system with 132 particles, for which all  $\eta$  values are accessible in the simulations. The agreement is satisfactory. Below  $\eta \approx -0.8$  the collapse is complete, with  $v=1$ .

Now for the thermodynamic quantities. Because of the linked-list problem, results are shown only for the  $N=132$  system. In Fig. 7 the data points are the molecular-dynamics results for the reduced temperature at various values of  $\eta$  for a rather dense system with  $\delta=4$ . The error bars are smaller than the symbols used for the data points. The value  $M=59$  listed in the figure follows from Eq. (57), and enables one to find the solution  $v=v_M^0(\eta)$  of the two-dimensional cell model. Equations (38) and (48) then result in the solid curve shown in the figure, where the tie lines of the cell model are included also.

In the homogeneous phase the agreement is satisfactory, but this is not amazing. Indeed, when  $\eta$  is sufficiently positive the particles can move freely and changes in energy will affect only the kinetic energy. The relation

$$T^* = \frac{K}{\epsilon N} = \frac{E - \Phi}{\epsilon N} = \frac{1}{2}N(\eta + \eta_0) \quad (60)$$

holds exactly, both for the ideal gas (with  $\eta_0=1/N$ ) and for the cell model (with  $\eta_0=1/M$ ). For the simulated system it holds asymptotically, with  $\eta_0$  apparently somewhat larger than  $1/M$ ; the same behavior was found in all the other simulated systems, irrespective of size and density. The small differences in  $\eta_0$  between the three

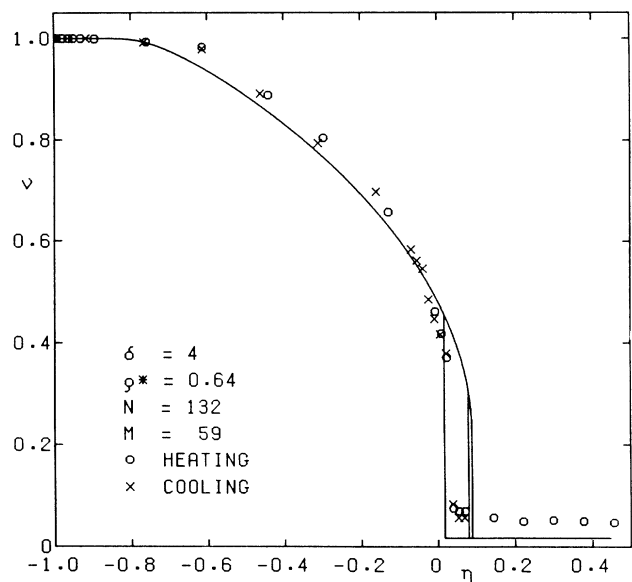


FIG. 6. The same as Fig. 5 but for a smaller system not restricted by linked-list overflow. Below  $\eta \approx -0.8$  the collapse is complete.

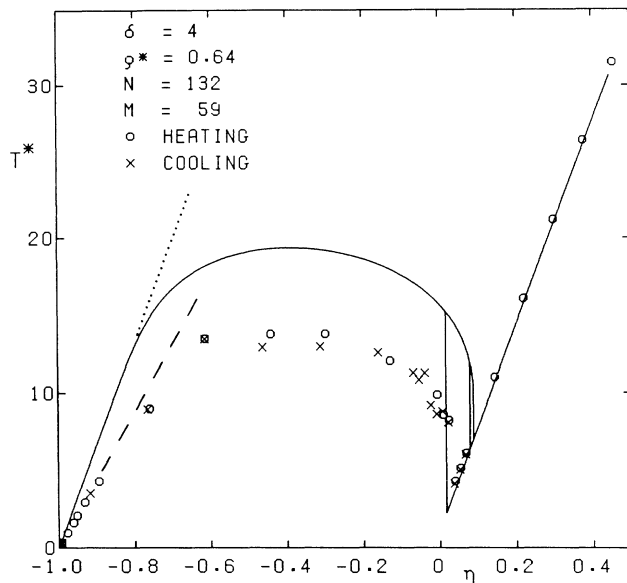


FIG. 7. The reduced temperature  $T^*$  as a function of  $\eta$  for a typical system. The data points are the molecular-dynamics results; the error bars are too small to be shown. The solid curve is the corresponding cell-model result. The independent particle result of Eq. (58) is shown by the dashed line for  $\delta=4$  and by the dotted line for  $\delta=\infty$ .

cases are due to the differences in the potential energy of a random configuration. Close to the end point of the homogeneous branch, just visible in the figure, one sees that  $T^*$  for the simulated system lies slightly above its linear asymptote. This premonitory phenomenon must be ascribed to transient clusters which decrease the aver-

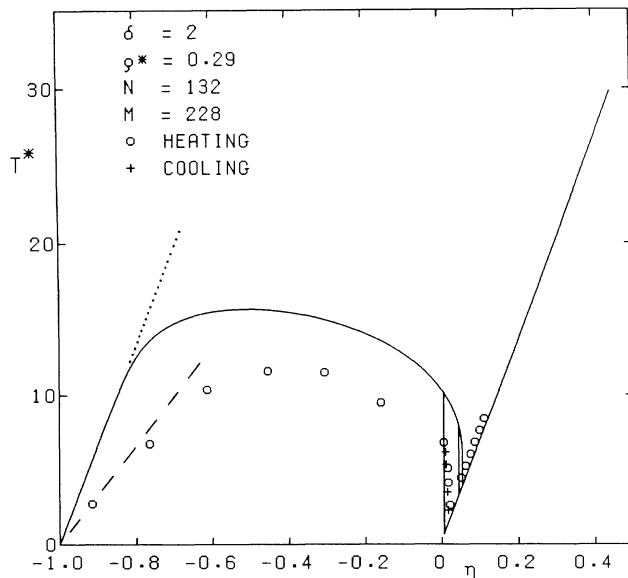


FIG. 8. The same as Fig. 7, but for a smaller density and for a pair potential that is less steep:  $\delta=2$ . For this value of  $\delta$ , equipartition holds in the completely collapsed state. Indeed, the slope of the corresponding dashed line is one-half of the slope of the dotted line belonging to  $\delta=\infty$ .

age potential energy below the value for a random configuration, increasing thereby the temperature.

In the collapsing phase the agreement is less satisfactory, although the phase transition occurs at the right place and although the qualitative features, including a region where  $\partial T^*/\partial \eta$  is negative, are similar. Again, the error bars are smaller than the symbols, but probably they are too flattering: in the collapsing phase, during a few test runs of  $\approx 10^6$  elementary time steps and especially at low densities, long relaxation times were encountered which reduce the efficiency of the simulation. The slow relaxation is probably due to two effects: the collapsing cluster is very compact and offers only a small cross section to the particles of the background, and any surplus energy in a collapsing cluster can be diverted among many internal degrees of freedom before it concentrates on a single particle which has to be kicked out in order for the system to approach equilibrium. These effects explain the small differences between results obtained in the sequence of runs with decreasing  $\eta$  and the results of the "heating" sequence. On the scale of the figure they do not turn up in the form of metastabilities. The metastable region seemed to be smaller for the simulated system than for the cell model, but definite conclusions could not be reached.

For  $\eta \lesssim -0.8$  in Fig. 7 (see also Fig. 6) the collapse is complete, both in the simulation system and in the cell model. The latter is again in a state where energy changes are passed on fully to the temperature. Equation (48) gives  $T^* = \frac{1}{2}N(\eta+1)$  for  $\nu=1$ , which is essentially the same as Eq. (60) if the difference in potential energy is taken into account. This also agrees with the independent-particle result of Eq. (58) for  $\delta=\infty$ , indicated by the dotted line in the figure. Insertion of  $\delta=4$  in Eq. (58) leads to the dashed line in the figure; now, the bottom of the collective well in which the particles are moving quasi-independently is not completely flat. The nice agreement between the dashed line and the simulation results for  $\eta < -0.8$  provides a check to the molecular-dynamics calculations and suggests that the difference in  $T^*$  in the collapsing phase between the cell model and the simulated system is mainly due to the different shapes of the respective pair potentials. This is supported by the good agreement found between  $N_c/N$  and  $\nu_M^0$ . That the rectangular well of the cell model is attached to space rather than to the particles probably has little influence; one could check this by simulating systems with higher values of  $\delta$ .

As a further example, Fig. 8 shows  $T^*$  for a system with  $\delta=2$  at a lower density. Here, and in the remaining figures, the error bars are again smaller than the symbols indicating the data points. The agreement in the homogeneous phase with the cell model and in the completely collapsed state with the independent-particle model is again satisfactory (in this case, the collective well is quadratic, equipartition holds, and the slope is half that for  $\delta=\infty$ ). Although the additional assumption  $N \gg M$  of the cell model is far from being obeyed in this case, the general agreement does not seem to suffer.

Results for the reduced pressure are compared in Fig. 9, obtained for the same system as in Figs. 6 and 7, in the

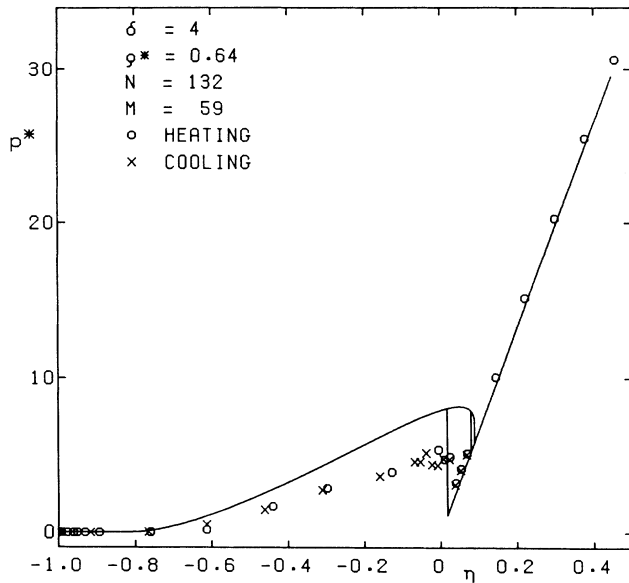


FIG. 9. The reduced pressure  $p^*$  as a function of  $\eta$  for a typical system. The data points are the molecular-dynamics results, and the solid curve is  $p_L^*$  of the corresponding cell model. In the collapsing phase the difference of  $p_M^* = T^*$  (see Fig. 7, drawn on the same scale) both with the data points and with  $p_L^*$  is large.

same computer experiments. The solid curve shows  $p_L^*$  of the cell model, given by Eqs. (40) and (49) in reduced form. In the homogeneous phase the agreement is again satisfactory, and also the difference with the ideal-gas law  $p_M^* = T^*$  of Eqs. (38) and (41) is small. In the collapsing phase  $p_M^*$  is still equal to  $T^*$ ; see Eqs. (48) and (50). Hence, to obtain  $p_M^*$  for the collapsing phase, the cell-model result for  $T^*$  in Fig. 7 can be copied in Fig. 9, which is drawn on the same scale. The difference with  $p_L^*$  is now large, due mainly to the factor  $(1-\nu)$  in Eq. (49). It is this factor which produces the horizontal part  $p_L^* = 0$  for  $\eta \lesssim -0.8$ , also found in the simulation.

Finally, an example for the specific heat, or rather its inverse, is shown in Fig. 10, again for the system of Figs. 6, 7, and 9. The solid curve represents Eqs. (39) and (51), the dashed line is Eq. (59) for  $\delta=4$ , and the dotted line is that equation for  $\delta=\infty$ . The scatter in the data points is considerable, although plotting  $1/C_V^*$  instead of  $C_V^*$  helped somewhat. It turned out that below  $\eta \lesssim -0.7$  the variance of the kinetic energy in Eq. (54) became too small to be calculated accurately by the DMDP. The corresponding data points had to be discarded. However, the approach around  $\eta \approx -0.6$  to the dashed line is convincing enough, in combination with the correct slope in  $\eta = -1$  of  $T^*(\eta)$  shown in Fig. 7. We conclude that the overall agreement is not bad, the specific heat being a rather sensitive quantity.

Only a few of the results obtained for the various quantities and systems can be shown here. Computer experiments for the other densities, both for  $\delta=2$  and 4, and also for the larger system with  $N=600$  were found to give a very similar picture. Since the cell model (apart from  $M$ , for which a reasonable *a priori* estimate was

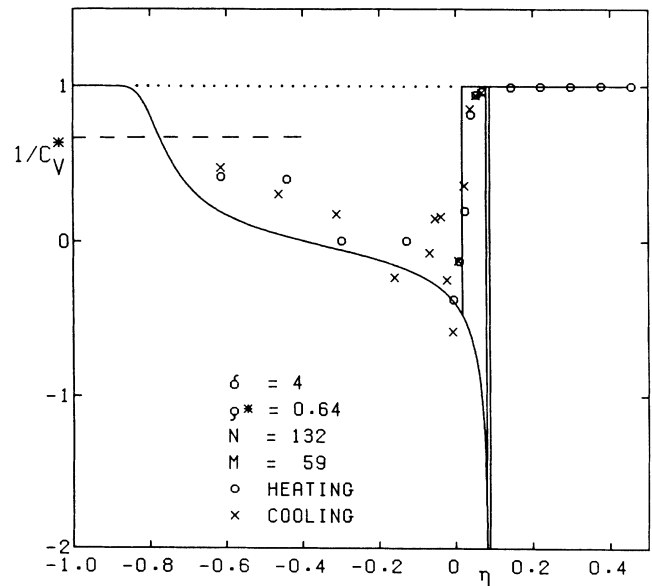


FIG. 10. The inverse of the reduced specific heat as a function of  $\eta$  for the same system as in Fig. 7. The data points are the molecular-dynamics results, and the solid curve is the cell-model result. The dashed line obeys Eq. (59) for  $\delta=4$ , the dotted line for  $\delta=\infty$ . Below  $\eta \approx -0.7$  no accurate data were obtained.

made) contains no parameter that can be fitted it performs remarkably well. A more general conclusion is that statistical mechanics can be applied successfully to systems of purely attractive particles, even though the stability condition is not obeyed—at least when the systems are finite.

### VIII. ASYMPTOTIC PROPERTIES

The correspondence between the predictions of the cell model and the properties of small systems with a true attractive-well pair potential suggests that also the asymptotic behavior, beyond reach in computer experiments, may be similar. If qualitatively important features of nonrelativistic self-gravitating systems are conserved when the pair potential of Eq. (2) is replaced by that of Eq. (3), then the asymptotic properties of the cell model may have some significance for cosmology.

When in the thermodynamic limit the scaling procedure of Hertel and Thirring<sup>9</sup> is followed, keeping  $N\epsilon$  and  $M$  together with  $N/L^d$  and  $E/N$  constant while  $N$  increases indefinitely, not only the homogeneous phase is extensive but also the collapsing phase. The entropy of Eq. (47) then is found to be an extensive quantity, and also the temperature, the pressure and the specific heat of Eqs. (48)–(51) behave as proper thermodynamic quantities should. That  $C_V$  is negative in a certain range of  $\eta$  values is somewhat unusual, but not impossible when energy instead of temperature is used as an independent variable. Hertel and Thirring showed also that use of the scaling procedure in the canonical ensemble leads to an

extensive free energy and prevents the occurrence of a complete collapse (except at  $T=0$ ) and of states with a negative specific heat. In short, by repairing the stability condition the scaling procedure leads to results that are in keeping with thermodynamics. However, the overall dependence on  $M$  remaining in the limit is somewhat arbitrary, and the manipulation of the parameters  $L$  and  $\epsilon$  characterizing range and strength of the pair interaction makes the scaling procedure into a mathematical artifact.

For the cell model the usual thermodynamic limit implies  $N \rightarrow \infty$  at constant values of  $E/N$ ,  $V/N$ , and  $M/N$ . The quantities  $L$  and  $\epsilon$  are also constant (but may be of the order of the spatial and energy scales of self-gravitating systems). In addition, the constant  $n \equiv N/M$  is taken to be very large. What happens to the collapsing phase in this limit?

Consider the effect on Eq. (43), assuming for the moment that  $\eta$  is a free variable. For  $-1 < \eta < 0$ , a solution of that equation in the limit  $M \rightarrow \infty$ , with both  $v_M^0$  and  $Mv_1^0$  of the order of 1, is possible only when the right-hand side diverges. Hence, the denominator in the left-hand side must vanish. Neglecting the term  $(M-1)v_1^2$  in the denominator one obtains the asymptote  $v = v_M^0 = (-\eta)^{1/2}$  of Eq. (46), shown in Fig. 2. Due to the logarithmic term, the convergence to this asymptote is exceedingly slow; even for  $M = 10^{12}$  the difference in  $v_M^0$  at  $\eta \approx -0.5$  still amounts to 6%.

Putting  $v = (-\eta)^{1/2}$  in Eq. (47) one discovers that the entropy per particle contains contributions proportional to  $\ln M$  or  $\ln N$ . A removal of these terms by way of a renormalization of the entropy would be quite arbitrary. Also, the use of  $\eta$  as a free variable in the limit amounts to keeping  $E/N^2$  constant rather than  $E/N$ . Consistent results with  $\eta$  as a free variable are only possible for finite systems, however large they may be.

When  $E/N$  is kept constant in the limit, irrespective of the value or even the sign of that constant, the system ends up at  $\eta=0$  with vanishing  $v_M^0$  and  $v_1^0$ , in the state where kinetic and potential energy are in complete balance. This is in contrast with the behavior in the canonical ensemble, in which, with  $T$  constant in the limit instead of  $E/N$  and now without the scaling procedure, the system is driven into the completely collapsed state at  $\eta = -1$ . The state at or around  $\eta=0$  cannot be reached by the canonical ensemble.

It is not difficult to show that the asymptotic behavior of the collapsing phase in  $\eta=0$  according to the micro-canonical ensemble is given, in crudest approximation, by

$$Nv_M^0(0) \approx \frac{dN}{\ln M}, \quad Nv_1^0(0) \approx \frac{N}{M}, \quad (61)$$

in terms of the number of particles in cell  $M$  (which could have been any cell, before renumbering) and their number in each of the other cells. The collapse is far from complete: although one cell takes a diverging amount of particles, this does not happen at the expense of the other cells!

Upon insertion of  $v = d/\ln M$  into Eqs. (47)–(50) the thermodynamic limit of the cell model appears not to exist. Of course, this is precisely what the stability condition is meant to prevent. The situation just stresses that

the thermodynamic limit (or, perhaps, rather the continuum limit<sup>5</sup> to which it is equivalent) is a useful technique to derive the “classical” or “continuum” thermodynamics of systems of macroscopic size, but cannot be applied to self-gravitating systems that are really large right from the outset. There is no reason, however, to reject Eqs. (47)–(50) for finite  $N$  and  $M$ , although when  $N$  and  $M$  are not extremely large, Eq. (61) may not be precise enough (whereas  $\eta=0$  may be too precise). The correction terms involved are of order  $\ln \ln M / \ln M$ , which means a deviation of 10% for  $M \approx 1.5 \times 10^{15}$  and of 5% for  $M \approx 2.6 \times 10^{43}$ , truly astronomical values.

The simultaneous presence in  $\eta \approx 0$  of the homogeneous and the collapsing phase suggests, in combination with the contraction into  $\eta \approx 0$  of the whole region of metastabilities (see Fig. 1), that for large  $N$  and  $M$  fluctuations occur between the two phases. Because of the matter transport that would be necessary, these fluctuations must be very slow. When the asymptotic result of Eq. (60) is valid, even approximately, it is hard to believe that these fluctuations could be restricted to a single cell at the time. As long as the background density  $N/M$  remains the same, almost any number of “collapsing” cells with  $dN/\ln M$  particles could be accommodated. Asymptotically, their mean spatial separation should increase, and the relaxation times involved would diverge strongly. The  $M$ -fold degeneracy of the entropy maximum should now be taken into account, and also the influence of premonitory phenomena in the homogeneous phase in  $\eta \approx 0$  may become important.

This picture can be supported by studying the eigenvalues  $\lambda = r$  and  $\lambda = s$  occurring in Eq. (30) in more detail, although a dynamical analysis of the cell model, in all its simplicity, will hardly be convincing. The cell model does not discriminate between neighboring cells and cells that are farther apart, to mention just one obstacle. Nevertheless, it is safe to conclude that the asymptotic time-dependent behavior of the model would destroy the very notion of equilibrium on which the calculations are based, and that a similar statement would hold *a fortiori* for a more realistic system. In the limit, an impasse is reached: in an infinite system that is not extensive anything can happen.

While being disastrous from a thermodynamical point of view, this may have interesting cosmological consequences, as we will argue. Consider, for definiteness, a large but finite system at  $\eta=0$ , described by the cell model. Not only are  $N$  and  $M$  large, but also  $L$ . Such a system would not be in equilibrium either, with the same averaged state being observed at any one moment in time. Rather, on the modest time scale available to an earthly cell-model watcher,  $\eta=0$  would correspond with a critical state taken from a degenerate ensemble of approximate maximum-entropy states. Precisely because the notion of equilibrium does not apply, the picture that was sketched has a certain cosmological appeal. We are even tempted to formulate a new cosmological principle, which, by being based on entropy considerations and because it is reminiscent of the anthropic principle (described e.g., by Rozenal<sup>15</sup> and Rosen<sup>16</sup>), is called *the entropic principle*: Very large systems of purely attractive

particles tend to be in a critical state characterized by  $\eta \approx 0$ , with slowly relaxing fluctuations of large amplitude that are rather localized in space.

Loosely speaking,  $\eta \approx 0$  seems to be likely for a really large system, although there is no *a priori* reason for such a state of affairs. However, if  $\eta$  were appreciably different from zero, equilibrium would be restored and the system should be found either, for  $\eta > 0$ , well inside a stable homogeneous phase or, for  $\eta < 0$ , well inside a stable collapsing phase with a single cluster against a diluted homogeneous background. In either case, the structure of the system would be much simpler than for  $\eta \approx 0$ , with much faster fluctuations of lesser amplitude. The similarity with the anthropic principle is evident.

Whether these speculations are of any use in cosmology or just are due to overstretching the significance of the cell model remains to be seen. It may be that a replacement of the artificial square-well potential by a true gravitational pair potential will completely destroy these simple and very qualitative conclusions. Leaving aside many other obvious criticisms that can be raised, one may, however, speculate that such a replacement would just enhance the structural complexity of the system at  $\eta \approx 0$ , by providing a hierarchy of spatial scales.

### IX. CONCLUSIONS

Molecular dynamics is a suitable method to study systems of particles with a purely attractive pair potential of short range. The results agree remarkably well with the predictions of the modified Hertel-Thirring cell model.

The stability condition is not necessary for an application of statistical mechanics. When it is not obeyed, relevant equilibrium properties of arbitrarily large but finite systems can be obtained by means of the micro-canonical ensemble. The canonical ensemble may give misleading results by exaggerating the significance of (almost) completely collapsed states.

In systems of purely attractive particles, a first-order transition accompanied by metastable states occurs between a homogeneous phase at high energies and a collapsing phase at low energies. The latter phase is characterized by the occurrence of a single, compact cluster containing a fraction of all particles. This phase is not extensive and may not be called thermodynamic: the thermodynamic limit does not exist for these systems. The phase transition takes place in a narrow region just above  $\eta = 0$ , where  $\eta = 2E/\epsilon N^2 - 1/N$  is the energy parameter that governs the behavior of the system.

The cell model suggests that when  $N$  is very large,  $\eta \approx 0$  is very likely. This leads to a new cosmological principle, *the entropic principle*: Large systems of purely attractive particles tend to be in a critical state, hesitating between homogeneity and a partial collapse.

### ACKNOWLEDGMENTS

It is a pleasure to thank P. H. E. Meijer for encouraging discussions, for preliminary calculations on one-

dimensional systems, and for bringing some of the references to our attention. A. F. Bakker allowed us to use the DMDP.

### APPENDIX: THE GROUND STATE

In the completely collapsed state, at  $T \approx 0$ , the particles are carrying out small independent oscillations in their collective well, which acts as an external field. This field is symmetric with respect to the center of mass, the motion of which is negligible and which is taken as origin. For this system, it is expedient to use the canonical ensemble. The canonical partition function is

$$Z_c = Q^N / \lambda^{dN} N! , \quad (\text{A1})$$

where  $\lambda = \hbar / (2\pi m k T)^{1/2}$  is the de Broglie wavelength, while

$$Q = \int_{V_0} d\mathbf{r} \exp(-\Phi / N k T) \quad (\text{A2})$$

is the configuration integral per particle. The collective well is

$$\begin{aligned} \Phi &= -\frac{1}{2} N(N-1) \epsilon \exp(-r^\delta / \sigma^\delta) \\ &\approx -\frac{1}{2} N(N-1) \epsilon (1 - r^\delta / \sigma^\delta) , \end{aligned} \quad (\text{A3})$$

where  $\delta$  is even and where use was made of  $r \ll \sigma$  for  $T \approx 0$ . The  $d$ -dimensional spherical volume  $V_0$  in Eq. (A2) is rather arbitrary; its radius should be large enough to catch all relevant oscillations. In the integral, the  $r$ -independent factor is moved up in front, and  $d\mathbf{r}$  is replaced by  $C r^{d-1} dr$ , where  $C$  is some constant. Finally, the integrand is scaled by substituting

$$y = (r/\sigma) [\frac{1}{2}(N-1)\epsilon/kT]^{1/\delta}$$

for  $r$ . The remaining integral can be taken over all  $y$ . One finds

$$Q = C' \frac{\exp[\frac{1}{2}(N-1)\epsilon/kT]}{[\frac{1}{2}(N-1)\epsilon/dT]^{d/\delta}} \int_0^\infty dy y^{d-1} \exp(-y^\delta) , \quad (\text{A4})$$

where  $C'$  is a new constant. The integral converges and is another constant. With the usual formulas for the free energy  $F \equiv -kT \ln Z_c$  and for the entropy  $S \equiv -\partial F / \partial T$ , one finds for the total energy

$$E \equiv F + TS = -\frac{1}{2} N(N-1) \epsilon + \frac{1}{2} d \left[ 1 + \frac{2}{\delta} \right] N k T . \quad (\text{A5})$$

Using  $\eta$  of Eq. (15) and taking  $d = 2$  one obtains Eq. (58) in the main text. In the thermodynamic limit, the free energy, the entropy, and the total energy, all taken per particle, diverge.

It may be noted that for  $\delta = 2$  the collective well of Eq. (A3) is harmonic, such that equipartition of energy holds; the resulting slope of  $T$  versus  $E$  is indeed half of that for the case  $\delta = \infty$ , corresponding to an ideal gas in a rectangular well.

- <sup>1</sup>D. Ruelle, *Hlev. Phys. Acta* **36**, 183 (1963).
- <sup>2</sup>M. E. Fisher, *Arch. Ration. Mech. Anal.* **17**, 377 (1964).
- <sup>3</sup>J. van der Linden, *Physica* **32**, 642 (1966); **38**, 173 (1968); J. van der Linden and P. Mazur, *ibid.* **36**, 491 (1967).
- <sup>4</sup>A. Münster, in *Proceedings of the International Conference on Thermodynamics, Cardiff, 1970*, edited by P. T. Landsberg (Butterworths, London, 1970), p. 293.
- <sup>5</sup>A. Compagner, *Am. J. Phys.* **57** (2), 106 (1989).
- <sup>6</sup>L. Spitzer, in *Dynamics of Star Clusters*, Proceedings of the 113th Symposium of the International Astronomical Union, 1984, edited by J. Goodman and P. Hut (Reidel, Dordrecht, 1985), p. 109.
- <sup>7</sup>D. Lynden-Bell, in *Gravitation in Astrophysics*, Vol. 156 of *NATO Advanced Study Institute, Series B: Physics*, edited by B. Carter and J. B. Hartle (Plenum, New York, 1987), p. 155.
- <sup>8</sup>L. van Hove, *Physica* **16**, 137 (1950).
- <sup>9</sup>P. Hertel and W. Thirring, *Ann. Phys.* **63**, 520 (1971).
- <sup>10</sup>N. G. van Kampen, *Phys. Rev.* **135**, A362 (1964).
- <sup>11</sup>M. Kac, G. E. Uhlenbeck, and P. C. Hemmer, *J. Math. Phys.* **4**, 216 (1963); **4**, 229 (1963); **5**, 60 (1964).
- <sup>12</sup>J. L. Lebowitz, J. K. Percus, and L. Verlet, *Phys. Rev.* **153**, 250 (1967).
- <sup>13</sup>A. F. Bakker, Ph.D. thesis, University of Delft (1983); H. J. Hilhorst, A. F. Bakker, C. Bruin, A. Compagner, and A. Hoogland, *J. Stat. Phys.* **34**, 987 (1984).
- <sup>14</sup>S. D. Stoddard, *J. Comput. Phys.* **27**, 291 (1978).
- <sup>15</sup>I. Rozental, *Big Bang Big Bounce: How Particles and Fields Drive Cosmic Evolution*, translated by J. Estrin (Springer-Verlag, Berlin, 1988).
- <sup>16</sup>J. Rosen, *Am. J. Phys.* **56** (5), 415 (1988).